

# Medium Access Control in Ad Hoc Networks with MIMO Links: Optimization Considerations and Algorithms

Karthikeyan Sundaresan, *Student Member, IEEE*, Raghupathy Sivakumar, *Member, IEEE*, Mary Ann Ingram, *Senior Member, IEEE*, and Tae-Young Chang, *Student Member, IEEE*

**Abstract**—In this paper, we present a new medium access control (MAC) protocol for ad hoc networks with multiple input multiple output (MIMO) links. MIMO links provide extremely high spectral efficiencies in multipath channels by simultaneously transmitting multiple independent data streams in the same channel. MAC protocols have been proposed in related work for ad hoc networks with other classes of smart antennas such as switched beam antennas. However, as we substantiate in the paper, the unique characteristics of MIMO links coupled with several key optimization considerations, necessitate an entirely new MAC protocol. We identify several advantages of MIMO links, and discuss key optimization considerations that can help in realizing an effective MAC protocol for such an environment. We present a centralized algorithm called *stream-controlled medium access* (SCMA) that has the key optimization considerations incorporated in its design. Finally, we present a distributed SCMA protocol that approximates the centralized algorithm and compare its performance against that of baseline protocols that are CSMA/CA variants.

**Index Terms**—Ad hoc networks, medium access control, MIMO links, stream control.

## 1 INTRODUCTION

Ad hoc networks or multihop wireless networks have typically been considered for use in military and disaster relief environments due to their capability to operate without any infrastructure support. In recent years, the use of the so-called “smart antennas” in ad hoc networks has gained consideration. The term “smart antennas” represents a broad variety of antennas that differ in their performance and transceiver complexity, such as the *switched beam* and the *digital adaptive array* (DAA) antennas.

A **switched-beam antenna** has a predetermined antenna array pattern that can be pointed to any of a small number of directions. The ability of such antennas to concentrate power in a certain direction provides a *directive gain* that can be used for extending range or reducing power. However, due to their simple signal processing capabilities, they are incapable of *adaptively* nulling out interference. Steered-beam antennas also have predetermined patterns, but they can be pointed to any of a near-continuous set of directions. This steering flexibility allows the array to track a user without incurring the “scalping loss” associated with switched beams [1], [2]. While steered-beam antennas are optimal in terms of signal-to-noise ratio (SNR) in free space with no interference, their performance deteriorates in a multipath environment where multiple copies of the signal can arrive from different directions [3]. An **adaptive array receiver** constructively combines the copies, yielding *array gain*, which is the factor increase in the average SNR equal to the number of antennas [4]. If the antennas are

sufficiently far apart, then the likelihood of the deepest fades is decreased, corresponding to *diversity gain*. Furthermore, an adaptive array receiver can attenuate the signal from an interference source (adaptive nulling). A transmit **digital adaptive array** can also provide array and diversity gains, augmenting those of a receiver array. It can transmit multiple cochannel data streams and, if channel state information (CSI) is available, each stream can have its own adapted pattern.

Smart antennas, in the conventional sense, are typically employed at only one end of the communication link, mostly at the access point or base station. Recently, the use of DAAs at both ends of the communication link has gained consideration, resulting in a technology popularly referred to as the *multiple input multiple output* (MIMO) technology. *Ad hoc networks with such MIMO links is the focus of this work.*

The presence of multiple elements at both ends of the link creates independent channels in the presence of multipath or rich scattering. Multiple independent data streams can be transmitted simultaneously on these different channels to provide extremely high spectral efficiencies (increase in capacity) that comes at the cost of no extra bandwidth or power [5]. This is referred to as *spatial multiplexing* and can be realized even without any channel state information (CSI) at the transmitter (e.g., BLAST [6]). Thus, while switched/steered beam antennas are ineffective in handling multipath [7] and fully adaptive array antennas merely mitigate the effect of multipath, MIMO links actually *exploit* multipath to provide the spatial multiplexing gain [4]. Furthermore, MIMO links are also capable of all the advantages provided by fully adaptive array antennas. We present more details on the specific advantages of MIMO in Section 2.

While MIMO carries significant promise and has been extensively researched in the physical layer research community [5], [8], [9], its flexibility and performance enhancement can be truly leveraged only by appropriately

• The authors are with the School of Electrical and Computer Engineering, Georgia Institute of Technology, Tech Tower, 225 North Avenue, Atlanta, GA 30332-0360. E-mail: {sk, siva, mai, key4078}@ece.gatech.edu.

Manuscript received 1 May 2004; revised 19 July 2004; accepted 21 July 2004. For information on obtaining reprints of this article, please send e-mail to: tmc@computer.org, and reference IEEECS Log Number TMCSI-0152-0504.

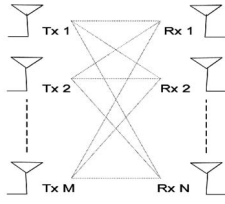


Fig. 1. MIMO Illustration.

designed higher layer protocols. At the same time, the key differences<sup>1</sup> and the physical layer properties of MIMO and switched beam antennas necessitate protocols that are very different from those developed for ad hoc networks with the latter class of antennas [10], [11]. Specifically, in this paper, we focus on the medium access control problem for ad hoc networks with MIMO links and consider the following questions:

- What are the key optimization considerations that should be incorporated in the design of a MAC protocol designed for the target environment?
- How can the versatile properties of MIMO links be leveraged to effectively realize a practical distributed MAC protocol with the optimal design?

While we systematically answer these questions later in the paper, we briefly use both results from related research at the physical layer and detailed arguments to identify several optimization considerations. Based on these considerations, we present both centralized and distributed MAC protocols called **SCMA** (Stream-Controlled Medium Access), for ad hoc networks with MIMO links. The centralized SCMA scheme serves both as a basis for the distributed SCMA design and as a benchmark for the latter's performance. Through packet level simulations, we show that distributed SCMA approximates the performance of the centralized scheme quite reasonably, while outperforming simple extensions of the CSMA/CA protocol for the target environment.

The rest of the paper is organized as follows: Section 2 provides some background on MIMO links. Section 3 highlights the key optimization considerations that are essential for the design of a MAC protocol for the target environment. Section 4 presents the centralized SCMA scheme. Section 5 describes the distributed SCMA MAC protocol for ad hoc networks with MIMO links. Section 6 presents the simulation results comparing SCMA with two baseline protocols. Section 7 discusses related work and Section 8 concludes the paper.

## 2 MIMO BACKGROUND

### 2.1 Relevant PHY Layer Characteristics

A MIMO link employs digital adaptive arrays (DAAs) at both ends of the link, as shown in Fig. 1. Such a link can provide three types of gain: array gain, diversity gain, and spatial multiplexing gain. Array and diversity gains primarily provide range extension, while spatial multiplexing gain primarily provides higher data rates.

Array gain can occur in an array receiver when the desired signal parts of each antenna output add coherently (coherent combining) and the noise parts add incoherently.

Array gain makes the average SNR at the output of the combiner (the average with respect to random multipath fading)  $N$  times greater than the average SNR at any one antenna element, where  $N$  is the number of antenna elements in the array. An array gain occurs even in the absence of multipath.

Diversity gain relates to the reduction in the variance of the SNR at the output of the combiner, relative to the variance of the SNR prior to combining. The reduction in variance depends on the diversity order, which in turn depends on the degree to which the multipath fading on the different antenna elements is uncorrelated. The maximum diversity order afforded by a MIMO link with  $M$  transmit antennas and  $N$  receive antennas is  $MN$ .

Since a wireless link is usually designed to have certain small probability that the SNR drops below some threshold value, both array and diversity gains contribute to range extension. In the presence of some channel state information, the factor of range extension  $d_f$  can approximately be given by [12],

$$d_f \approx \left\{ \left( \sqrt{M} + \sqrt{N} \right)^2 \right\}^{\frac{1}{p}}, \quad (1)$$

where  $p$  is the path loss component. While array gain continues to grow as more antennas are added, diversity gain tends to diminish, like the reduction in the variance of a sample mean. However, for a transmit array to provide either array or diversity gain, the data streams transmitted from the different antenna elements must be dependent.

In the presence of multipath or rich scattering, the MIMO link can provide spatial multiplexing gain. This gain is defined as the asymptotic increase in the capacity of the link for every 3 dB increase in SNR [13]. This gain can be achieved when the transmit array transmits multiple independent streams of data. In the simplest configuration, the incoming data is demultiplexed into  $M$  streams and each stream is transmitted out of a different antenna with equal power, at the same frequency, same modulation format, and in the same time slot. In fact, this approach is optimal in terms of capacity when the transmitter array has no CSI [5]; hence, the approach is often referred to as open-loop MIMO (OL-MIMO). At the receiver array, each antenna receives a superposition of all of the transmitted data streams. However, each stream generally has a different "spatial signature" and these differences are exploited by the receiver signal processor to separate the streams. When  $M = N = k$ , the asymptotic capacity is given by the following equation [4]:

$$C \approx k \log_2(1 + \rho), \quad (2)$$

where  $\rho$  represents the average SNR at any one receive antenna.<sup>2</sup>

On the other hand, when the multiple antennas are used only for array and diversity gain, the asymptotic capacity is

$$C \approx \log_2(1 + \rho'), \quad (3)$$

where  $\rho'$  is a random SNR with a mean that increases only linearly with the array gain and a variance that decreases with the diversity order. Therefore, the capacity grows linearly with  $k$  with spatial multiplexing, but only logarithmically with array and diversity gain. *Thus, our focus in this*

2. Correlation in the multipath fading across the antenna elements because of inadequate interelement spacing leads to a reduction in the factor  $k$  [14].

1. We elaborate more on the differences in Sections 2 and 3.

work is to exploit the spatial multiplexing gain to increase the capacity of the system. However, we show later that the range extension possible through the diversity gain can be intelligently leveraged to address some key problems at the MAC layer. Further, (2) and (3) only indicate the advantage of spatial multiplexing over diversity and array gains from the perspective of a single link using Shannon bounds. Hence, we also investigate the relative aggregate throughput gains between using spatial multiplexing for capacity and diversity for range extension from the network's perspective in the Appendix. We show that, even from the network's perspective, it pays off to use spatial multiplexing instead of diversity for obtaining higher throughput gains.

Another degree of classification of MIMO links is based on whether or not the transmitter uses CSI with respect to the receiver. If CSI is used at the transmitter, the MIMO link is referred to as closed-loop MIMO (CL-MIMO). CL-MIMO is known to outperform OL-MIMO under conditions of low SNR, correlated fading, and interference [15], [16], [17], [14]. Since we are considering improvements to network throughput where interference between MIMO links is allowed, we consider CL-MIMO. While we assume that OL-MIMO is used for MAC layer control packet exchanges (e.g., Request-to-send and Clear-to-send messages in the CSMA/CA framework) due to the absence of CSI at the transmitter initially, we leverage these packet exchanges to exchange the CSI,<sup>3</sup> thereby enabling the use of CL-MIMO for the actual data packet transmission.

## 2.2 Abstraction

We use the following abstraction and assumptions for the PHY layer in our work. We assume that all the nodes in the network employ DAAs with the same number of elements ( $M = N = k$ ), and operate on a single channel. The signals sent on the different modes of the channel represent the different streams transmitted. The total number of elements at a node correspond to the total available resources or *degrees of freedom* (DOFs) at the node. We assume that each receiver array treats all interference as noise. This is consistent with practical linear multiuser detection schemes such as minimum mean squared error (MMSE) [4].<sup>4</sup> In a MIMO link, a receiver can isolate and decode all the incoming streams successfully as long as the total number of incoming streams ( $n$ ) is less than or equal to its DOFs ( $n \leq k$ ). On the other hand, if the incoming streams overwhelm the DOFs at the receiver ( $n > k$ ), it will not be possible to decode any of the desired signal streams, if the excess ( $n - k$ ) streams degrade the  $k$  streams below their receive threshold. However, if the strength of the excess (say, interfering) streams is far weaker than that of the desired ( $k$ ) streams such that the desired streams can still be received with at least the receive threshold, then it may be possible to decode the desired streams [17]. In terms of transmission, a transmitter can use up all the available DOFs (taking into account DOFs available at nodes in the neighborhood after they have suppressed any interference) to spatially multiplex signals.

3. The actual information can be achieved using several conventional PHY layer training mechanisms [18].

4. The capacity of such a link when interference is present is found by first whitening the channel and then applying the usual capacity formulas.

## 2.3 PHY Layer Flexibility

We now briefly outline the characteristics that are unique to MIMO and potentially relate to designing and realizing an efficient MAC protocol:

- *Adaptive Resource Usage.* In the case of MIMO, any resource not spent in suppressing interference can be dedicated either to increasing the gain on the existing streams or to increasing the number of streams for the desired transmission as long as there are enough resources available at both ends of the link. In contrast, switched beam antennas provide only directive gain in a point-to-point link; they cannot provide spatial multiplexing.
- *Tx Range versus Capacity Trade Off.* Instead of splitting the data stream into  $k$  parallel independent streams and transmitting them simultaneously on  $k$  elements to achieve multiplexing gain, dependent streams can be transmitted on multiple elements to achieve transmit diversity gain. Note that diversity gain does not require multiple elements to be present at both the transmitter and receiver. This diversity gain can provide us with *range extension* (a larger transmission range) or *power minimization*, or *better link reliability*, as desired. Furthermore, suppression of dependent interference streams requires fewer DOFs than suppression of independent streams.
- *Flexible Interference Suppression.* Irrespective of the location of the interference sources, receivers in a multipath environment with MIMO links can suppress interfering streams as long as they have a sufficient number of DOFs to do so. In the worst case, even in the presence of  $k - 1$  interfering streams, a receiver with  $k$  elements can still receive a desired data transmission transferred on a single stream (provided the presence of multipath causes the signals to fade independently). This is in contrast to switched beam antennas, where interference sources in the same beam as the desired signal can simply not be tolerated.
- *Robustness to Multipath Fading.* MIMO does not require *line of sight* (LOS) and can leverage multipath productively. Hence, it can be applied to rich scattering and multipath environments which are very common indoors. In contrast, for effective operation, switched beam antennas require an LOS path between the transmitter and receiver because they are not optimized for multipath effects. This presents a major obstacle in using these antennas in multipath environments where the desired signal can arrive from multiple directions. On the other hand, any channel gain possible through the use of multiple elements is degraded if the angular spread of the desired signal multipath is larger than the beam-width.

The advantages outlined above demonstrate the potential benefits that can be gained by employing MIMO. In the next section, we outline the key optimization considerations that need to be taken into account in order to realize an efficient MAC protocol for the target environment.

## 3 MOTIVATION

CSMA/CA (Carrier Sense Multiple Access with Collision Avoidance) is the de facto MAC protocol considered for use

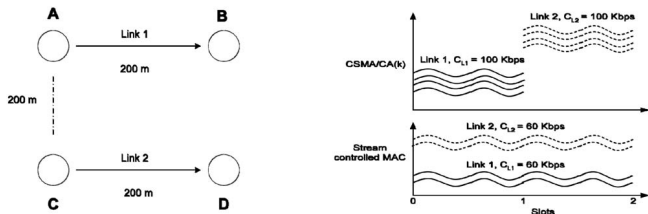


Fig. 2. Stream control topology.

in ad hoc network environments. Interestingly, a simple extension of CSMA/CA for MIMO links can be realized that can provide a  $k$ -fold improvement in throughput performance through spatial multiplexing ( $k$  is the number of elements at each node), compared to a pure omnidirectional environment.

We refer to the simple extension to CSMA/CA as CSMA/CA( $k$ ). Essentially, CSMA/CA( $k$ ) works in the exact same fashion as CSMA/CA, except that *all* transmissions are performed using  $k$  streams to tap the spatial multiplexing gain. Such a protocol, when compared to default CSMA/CA operating in the same network topology, but with omnidirectional antennas, will achieve close to  $k$  times the throughput performance as the latter.<sup>5</sup> While a  $k$ -fold is indeed quite attractive, the question that we answer in this section is: *Is it possible for a more intelligent MAC scheme to realize better performance?* More importantly, does the degree of improvement justify the development of a new MAC scheme, instead of using a protocol such as CSMA/CA( $k$ )? We argue that the answers to both of the questions is *yes*. We discuss why CSMA/CA( $k$ ) does not truly leverage the capabilities of MIMO using simple toy topologies. More importantly, we show in Section 6 that the difference in performance between the “unaware” CSMA/CA( $k$ ) scheme and MIMO “aware” MAC scheme increases with an increasing number of antenna elements.

In the rest of the section, we outline the key optimization considerations that need to be accounted for in the MAC design in order to effectively utilize the capabilities of MIMO.

### 3.1 Stream Control Gains

When a link is allowed to use only a subset of the maximum possible number of streams (say  $m$  out of  $k$ ), it can distribute its transmit power over just the  $m$  strongest channel modes (streams). Thus, when compared to two interfering links operating using TDMA at the maximum number of streams  $k$ , letting the links operate simultaneously but with  $\frac{k}{2}$  streams will result in improving the overall utilization in the network. We term the gains achievable through such simultaneous operation of interfering but stream controlled links as *stream control gains*.

In the simple toy topology shown in Fig. 2 where the nodes have four-element DAAs each, consider transmissions from node A to node B and from node C to node D. CSMA/CA( $k$ ) allows only one transmission to take place in a given time slot, but the transmission proceeds with all the four streams. On the other hand, consider a stream-controlled MIMO MAC where the two transmissions proceed simultaneously but the number of streams transmitted by each node is optimized (in this case to two streams) to give the maximum overall network throughput (Fig. 2). For this simple two link topology, an improvement

of 20 percent can be obtained in capacity over that of a TDMA scheme [16]. In general, as the number of mutually interfering links ( $l$ ) increases, the subset of streams used by each of the links decreases ( $\frac{k}{l}$ ), which in turn increases the gain obtained from performing stream control.

In a CL-MIMO system, there is a one-to-one mapping between streams and transmit array weight vectors; with the help of CSI, each antenna element transmits a superposition of all (weighted) data streams. In the receiving node, there will be a different array weight vector for each stream. Therefore, there will be a channel gain for each stream, which is the stream gain. These *stream gains are not equal* and, for moderate-to-low SNR, they can *have quite large disparities*, even in the presence of interference [16]. This in turn motivates the need for performing stream control in order to increase the network utilization, wherein the best possible channel modes (two in the above example) are selected for transmission. In the above example, the normalized gains of 1, 0.9, 0.7, and 0.6 were assumed on the four streams. Hence, during stream control, the two best streams with gains of 1 and 0.9 were chosen by the two links to provide an improvement of around 20 percent. The improvement of 20 percent is quite conservative for equal powered transmitters in the presence of low correlation between the desired and interfering MIMO streams based on the studies in [19]. In fact, [19] shows that up to a 65 percent performance improvement over a TDMA scheme can be obtained from performing stream control for measured indoor channels in the presence of low correlation. We summarize the above discussions by the following observation:

**Observation 1.** *Multiple interfering links operating simultaneously using stream control achieve better overall throughput performance when compared to a scenario in which they operate using TDMA and  $k$  streams each.*

### 3.2 Partial Interference Suppression

When two interfering links are positioned such that the interference signals traverse a longer distance ( $R$ ) than the desired signals ( $D$ ) with  $1 \leq \frac{R}{D} \leq 2$ , the improvement of MIMO with stream control over CSMA/CA( $k$ ) can increase significantly.<sup>6</sup> This is due to the flexible interference suppression capabilities provided by DAAs. The amount of resources that need to be sacrificed (expended) at a node to suppress an interference depends on the actual strength of the interference and the degree of spatial correlation [4], [16].

This is better illustrated through the toy topology in Fig. 3, where the nodes have a four-element DAA each. Consider three transmissions, from node A to node B, from node C to node D, and from node E to node F. CSMA/CA( $k$ ) allows only one of the transmissions to take place in any time slot, but on all four streams. Consider a stream-controlled MIMO MAC where the nodes operate with two streams each. Now, the transmitters C and E are outside the receive range but within the carrier-sensing range of receiver B. Hence, the number of DOFs required to suppress interference at node B in this case might only be a fraction of the total number of interfering streams, which in turn depends on the strength of the interfering streams and their spatial correlation. Assuming this fraction to be half, this allows the three transmissions to take place simultaneously on two streams each (Fig. 3). Hence, fewer resources are

6. We consider  $\frac{R}{D} \leq 2$  since CSMA/CA (e.g., IEEE 802.11b) and, hence, CSMA/CA( $k$ ) assumes no interference from signals whose  $\frac{R}{D} > 2$ .

5. Some tuning of the constant intervals used by CSMA/CA is essential.

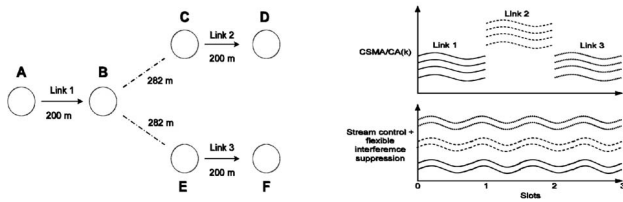


Fig. 3. Partial interference suppression topology.

required to suppress interference when the interfering signals are from far away than when they are from close by. This, in turn, results in more of the resources at a node being available for improving the performance of the desired transmissions/receptions.

But, it must be noted that additional resources can be made available at any node due to flexible interference suppression, only as long as the node operates on a subset of the maximum number of streams possible. This is because, if the node operates on all available streams, then it will have to expend all its resources to receive desired signal streams from its intended receiver. Hence, no additional resources will be made available in this case. Thus, *the gain of flexible interference suppression can be obtained only in conjunction with stream control*. This explains why CSMA/CA(k) cannot exploit the advantage of flexible interference suppression, even if its mechanism of silencing nodes in the two hop neighborhood of any transmission is extended to incorporate flexible interference suppression.

In the above example, the average number of streams/slot is six for a stream-controlled MAC, while it is only four for CSMA/CA(k). Also, it has been shown in related work that the performance gain over a TDMA-based approach, obtained by employing flexible interference suppression can be as high as 65 percent for a simple two link topology [19]. Based on the above discussions, we make our second observation:

**Observation 2.** *The flexible interference suppression capabilities of DAAs helps create additional resources at a node that can be used in conjunction with stream control for additional transmissions (receptions) to provide additional gain.*

### 3.3 Receiver Overloading

While the above two factors directly help a MIMO aware MAC achieve improved performance over CSMA/CA(k), there exists one facet of MIMO that can potentially *degrade* its performance when compared to CSMA/CA(k). In CSMA/CA(k), since there can be only one active transmitter in any *contention region*, the other passive receivers in the same region can be *overloaded* with more streams than they can receive. This paves the way for spatial reuse. Hence, if a passive receiver belongs to more than one otherwise nonoverlapping contention regions, then there can be an active transmitter in each of those contention regions.

On the other hand, in a MIMO MAC employing stream control, all the transmitters within a contention region use the best subset of their streams such that no receiver in the region is overloaded. But, if any of the receiver nodes also belong to other contention regions, then this prevents the nodes of those other contention regions from transmitting since this will overload the active receiver. This in turn reduces the advantage of spatial reuse and could potentially degrade performance.

For example, consider the simple topology in Fig. 4. There are four links, namely, L1, L2, L3, and L4. The link L1

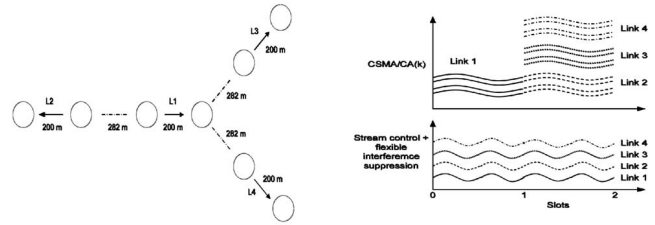


Fig. 4. Receiver overloading topology.

interferes with L2, L3, and L4, but the latter three links do not interfere with each other. If four element DAAs are used, CSMA/CA(k) can schedule L1 during one slot with four streams and L2, L3, and L4, during the next slot with four streams each. Thus, the average throughput in the network in terms of streams per slot is eight. However, if a stream-controlled MIMO MAC is used, all four links will operate with exactly one stream each as any more streams will overload the receiver of link L1. Thus, the average throughput obtained is just four, which is smaller than that of CSMA/CA(k) (Fig. 4). Further, this degradation would increase as the number of passive receivers (belonging to multiple contention regions) increases, and also as the number of contention regions that a passive receiver belongs to increases. We attribute the above advantage of CSMA/CA(k) to its ability to perform *receiver overloading*, i.e., a *passive* receiver can be exposed to more than the maximum number of interfering streams. Thus, our final observation is:

**Observation 3.** *The inability to overload a passive receiver because of performing pure stream control could result in a performance degradation that outweighs the gains from stream control.*

## 4 CENTRALIZED SCMA

In this section, we present the centralized *stream-controlled medium access* (SCMA) protocol for ad hoc networks with MIMO links. The design of a centralized algorithm has two potential benefits: 1) It provides a basis for the design of the distributed algorithm and 2) it serves as a benchmark against which the distributed algorithm can be compared.

The centralized algorithm has the objective of maximizing the network utilization subject to a given fairness model. The fairness model that we employ is the proportional fairness model. A good exposition on the motivation for the fairness model can be found in [20]. While the primary goal is to come up with a channel allocation vector that is proportionally fair, the maximization of the network utilization can be achieved only by realizing the optimization considerations identified in Section 3. Thus, the centralized algorithm attempts to leverage the benefits of stream control and partial interference suppression, while at the same time enabling the receiver overloading possible in CSMA/CA.

### 4.1 Insights and Overview

The basis of the centralized SCMA algorithm rests on an observation about the (lack of) a receiver overloading problem: There exists a specific subset of links in the network that contributes to the lack of receiver overloading when performing pure stream control. An example of such a link is Link 1 in Fig. 4. We refer to such links as *bottleneck links*. An alternative description for bottleneck links is that

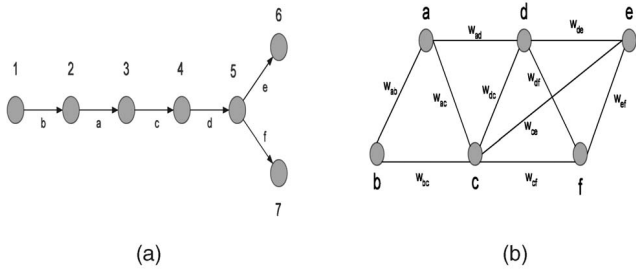


Fig. 5. Graphs. (a) Network topology and (b) flow contention graph.

they belong to *multiple contention regions* in the network. It can be observed in Fig. 4 that Link 1 belongs to three contention regions with links 2, 3, and 4 respectively.

If such bottleneck links are scheduled in the nonstream controlled fashion (operating on all  $k$  streams), such links can essentially be removed from further scheduling considerations, leaving the scheduling algorithm with only independent contention regions within which pure stream control can be employed. Upon closer look, it can further be observed that the bottleneck links can be identified by identifying vertices in the *flow-contention graph*<sup>7</sup> of the underlying network that belong to multiple maximal cliques.

The centralized SCMA algorithm is designed to achieve not just proportional fairness, but also to incorporate the above insights, and hence has the following key elements:

1. identifying bottleneck links (link classification)—referred to as *red* links in the algorithm,
2. obtaining the proportional fair allocation, and
3. scheduling to achieve the proportional fair allocation.

The scheduling component involves 1) scheduling of bottleneck (red) links in a nonstream controlled manner and 2) scheduling of the nonbottleneck (white) links in the network based on pure stream control.

## 4.2 Centralized Algorithm

We now present the centralized algorithm, the pseudocode for which is presented in Fig. 7. We also use a running example of the network topology in Fig. 5a to illustrate the different stages of the algorithm.

### 4.2.1 Graph Generation

Given the network topology  $G = (V, E)$ , where  $V$  represents the set of nodes in the network and  $E$  represents the communication links (Fig. 5a), the *flow contention graph*  $G' = (V', E', W)$  is generated (Fig. 5b), where  $V'$  represents the set of links in the network (Step 1).  $E'$  represents the edges between any two vertices in  $G'$ , whose links contend with each other in the underlying network, and the weight of the edge ( $\epsilon W$ ) represents the amount of interference caused by one link on the other.

Before being able to classify the vertices, it is necessary to identify all the nonoverlapping contention regions in the link contention graph. This is equivalent to the problem of identifying all the maximal cliques in  $G'$ . We next explain how this can be achieved.

7. A graph with vertices representing links in the underlying network and an edge between two vertices existing if the two corresponding links contend with each other in the underlying network [20].

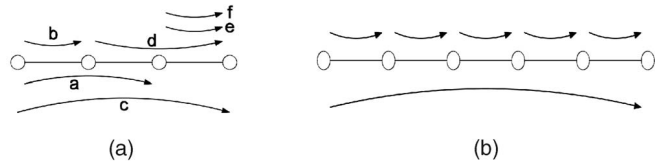


Fig. 6. Wireline flow contention topologies.

### 4.2.2 Clique Identification and Coloring

Identifying all the maximal cliques in a graph is known to be an NP-Hard problem. Hence, the centralized algorithm makes use of an algorithm that determines all the maximal cliques in chordal graphs (having less than four cycles). It first determines the *perfect elimination ordering* (PEO) using LexBFS (Lexicographic Breadth First Search) [21] for the chordal graph and then applies a *linear* algorithm that detects all the maximal cliques given the PEO using a theorem by Fulkerson and Gross [22].

Though the algorithm only works for graphs having cycles of size less than four, note that the graph in our case corresponds to the flow contention graph. Hence, for a cycle of size four to be present in the flow contention graph, a cycle of at least size eight must be present in the node graph with no nodes being present inside the cycle. Given the typical size of ad hoc networks to be of the order of 1,000-1,500m in either dimension with about 50-200 nodes randomly and uniformly distributed, the probability of finding such a scenario is very low. Hence, we use this algorithm to determine all the maximal cliques in the flow contention graph.

Once all the maximal cliques have been obtained, the vertices (in  $G'$ ) are then colored as follows (Step 2): The number of maximal cliques that each vertex (link) belongs to is recorded as its clique degree ( $d$ ). All vertices that belong to more than one maximal clique (bottleneck links,  $d > 1$ ) are colored “red,”<sup>8</sup> while the vertices belonging to a single maximal clique are colored “white”<sup>9</sup> (lines 1 and 2). In the example in Fig. 5, the different maximal cliques in Fig. 5b are  $cdef$ ,  $abc$ , and  $acd$ . Hence, vertices  $c$ ,  $d$ , and  $a$  are colored red while the rest are colored white.

### 4.2.3 Obtaining Proportional Fair Allocation

The analogy of a contention region in a wireless domain is a bottleneck link in a wired domain. Hence, the problem of finding the proportional fair allocation in wireless networks with links belonging to multiple contention regions is the same as the corresponding problem in wireline networks with flows passing through multiple bottleneck links. For example, our wireless flow contention graph in Fig. 5b can be mapped to the wireline flow contention topology in Fig. 6a. For the popular example in Fig. 6b with  $n$  single-hop flows and one  $n$ -hop flow ( $n$  bottleneck links with a bandwidth of one), the proportional fair allocation is  $\frac{1}{n+1}$  for the long flow and  $\frac{n}{n+1}$  for each of the short flows [23]. Thus, the longer flow that passes through multiple bottlenecks has the potential of sacrificing its own utility for a greater return in terms of the sum of the utilities gained by all the flows. This is an important aspect in obtaining the proportional fair allocation (Step 3). However, to extend the solution to generic topologies, one needs to rank the flows

8. A red vertex in  $G'$  corresponds to a red link in the network.

9. A white vertex in  $G'$  corresponds to a white link in the network.

```

INPUT: Network Topology graph G = (V,E), and K
      V = nodes in the network
      E = pair of nodes within reception range of each other
      K = number of antenna elements at each node
Step1: First generate the Flow Contention Graph G' = (V',E')
      from G based on neighborhood properties
Step 2: Color the vertices in G' (links in G); COLOR(G')
Step 3: Obtain the proportional fair rate allocation: RATE.ALLOC(G')
Step 3: Obtain the proportional fair schedule : SCHEDULE(G')

COLOR(G')
1 Obtain the clique degree (d) of each link
2  $\forall i \in V'$ , If  $d(i) > 1$ , add  $i$  to set RED
   else add  $i$  to set WHITE

RATE.ALLOC(G')
3  $\forall i \in \text{RED}$ , rank the link based on  $(p(i))$ , set  $rate_i = 0$ 
4  $C \rightarrow$  set of all maximal cliques in  $G'$ ,  $\forall c \in C$ ,  $resource(c) = 1$ 
5  $J = \text{RED}$ 
6 Do While ( $J \neq \emptyset$ )
7   Find  $k = \arg\{\min(rank_i)\}$ , where  $i \in J$ 
8    $rate_k = \min(\frac{\min\_resource_1}{p(k)}, \min\_resource_2)$ 
9    $\forall c \in M(k)$ ,  $resource(c) = resource(c) - rate_k$ 
10   $J = J - \{k\}$ , re-rank  $i$ ,  $\forall i \in J$ 
11  $\forall j \in \text{WHITE}$ ,  $rate_j = \frac{resource_c}{num\_whitelinks(c)}$ , where  $c = M(j)$ 

SCHEDULE(G')
12 Obtain L,  $\forall i \in V'$ ,  $service_i = 0$ ,  $slot.index = 0$ 
13  $\forall i \in V'$ ,  $l_i = rate_i \cdot L$ ,  $request_i = l_i \cdot K$ 
14  $\forall i \in V'$ ,  $res_i = K$ ,  $alloc_i = 0$ 
15 Do While ( $(i = \text{Get.Red}()) \neq \emptyset$ )
16   $service_i = service_i + K$ ,  $alloc_i = K$ ,  $request_i = request_i - K$ 
17   $\forall k \in \text{Neighbor}(i)$ ,  $res_k = res_k - w_{ik} \cdot K$ 
18 Do While ( $(j = \text{Get.White}()) \neq \emptyset$ )
19   $service_j = service_j + 1$ ,  $alloc_j = alloc_j + 1$ ,  $request_j = request_j - 1$ 
20   $\forall k \in \text{Neighbor}(i)$ ,  $res_k = res_k - w_{ik}$ 
21  $slot.index ++$ ,  $\forall i \in V'$ ,  $alloc_i = 0$ ,  $res_i = K$ 
22 If  $(\text{mod}(slot.index, L) = 0)$ ,  $\forall i \in V'$ ,  $request_i = l_i \cdot K$ 
23 Goto line 15

Get.Red()
24 Find  $D \subseteq \text{RED}$ , such that,  $\forall m \in D$ ,  $request_m > 0$ , &&  $res_m = K$  &&
   ( $res_n \geq w_{mn} \cdot K$ ,  $\forall n \in \text{Neighbor}(m)$ , &&  $alloc_n > 0$ )
25 Return  $i = \arg\{\min(rank_m)\}$ , where  $m \in D$ 

Get.White()
26 Find  $D \subseteq \text{WHITE}$ , such that,  $\forall m \in D$ ,  $request_m > 0$ , &&  $res_m = 1$  &&
   ( $res_n \geq w_{mn}$ ,  $\forall n \in \text{Neighbor}(m)$ , &&  $alloc_n > 0$ )
27 Return  $j = \arg\{\min(service_m)\}$ , where  $m \in D$ 

```

Fig. 7. Pseudocode for the centralized algorithm.

passing through multiple bottlenecks (links belonging to multiple contention regions or red links) based on their potential to bring higher returns in terms of aggregate network utility and the allocation would start with the flow (red link) having the highest potential.

In the rest of the discussions, let  $j$  represent the red link under consideration,  $i$  and  $j$  be the indices used to represent links, and  $c$  and  $d$  be the indices used to represent the maximal cliques (contention regions). Further, let  $M(i)$  correspond to the set of maximal cliques that the link  $i$  belongs to (e.g.,  $M(a) = \{abc, acd\}$  in Fig. 5b<sup>10</sup>) and  $L(c)$  correspond to the set of links that belong to the contention region  $c$ . For the purpose of ranking, every red link ( $j$ ) has an attribute, namely, "potential degree" ( $p(j)$ ).  $p(j)$  corresponds to the cardinality of the set of links  $P_j$ , where

$$\forall i \in P_j, \{M(i) \subseteq M(j)\} \parallel \{ (M(i) \subseteq M(j)) \& (M(i) \cap M(j) \neq \emptyset) \& (C_1 \parallel C_2) \}, \quad (4)$$

where  $C_1$  and  $C_2$  represent the following constraints,

$$C_1 \rightarrow \forall c \in \{M(i) \setminus M(j)\} : L(c) = \{i\} \quad (5)$$

$$C_2 \rightarrow \exists c \in \{M(i) \cap M(j)\} : (\exists k \in P_j \& k \in L(c) : \forall d \in M(k), L(d) \setminus \{i, j, k\} = \emptyset). \quad (6)$$

The role of the operator  $\setminus$  in  $A \setminus B$  is to isolate the elements in set  $A$  that are not in set  $B$ . The set  $P_j$  includes all links that contend with red link  $j$  and are capable of exploiting a sacrifice in  $j$ 's utility to increase the aggregate utility in return.  $p(j)$  is hence indicative of the available potential (number of links that can gain in utility) for resulting in better aggregate utility for a sacrifice in utility by  $j$ . While all links whose maximal cliques are a subset of those of  $j$  ( $M(i) \subseteq M(j)$ ) are obvious members of  $P_j$ , even some links that contend with  $j$

( $M(i) \cap M(j) \neq \emptyset$ ) and whose maximal cliques are not a subset of those of  $j$  (referred to as "border" links, e.g., link  $a$  is a border link for red link  $d$ ), can be members of  $P_j$  under constraints  $C_1$  or  $C_2$  or both. At a high level, the two constraints identify only those border links that will be able to directly or indirectly exploit the utility sacrificed by  $j$ . Specifically,  $C_1$  identifies border links that can directly exploit the utility sacrificed by  $j$  due to the absence of any contending link in all its contention regions of which  $j$  is not a member.  $C_2$ , on the other hand, identifies those border links that can indirectly help exploit the sacrificed utility even though they may not be able to directly exploit it. For the border links to help indirectly, there must be a link belonging to  $P_j$  and contending with the border link such that it can directly exploit the utility sacrificed by  $j$  in the event that the border link is not able to exploit it. In our example, the red links have the following potential degrees:  $p(c) = 6$  with  $P_c = \{a, b, c, d, e, f\}$ ,  $p(d) = 3$  with  $P_d = \{d, e, f\}$ , and  $p(a) = 2$  with  $P_a = \{a, b\}$ .  $P_d$  does not include border links  $a$  and  $c$  since they do not satisfy both the constraints. Similarly,  $P_a$  does not include links  $c$  and  $d$ .

The red links are ranked based on the potential degree with the red link having the highest potential degree ranked first (minimum rank) (line 3). In the example in Fig. 5b, link  $c$  obtains the highest rank, followed by  $d$  and  $a$ .

Once the red links are ranked, we start with the highest ranked link ( $c$ ) that has the maximum potential for increasing the aggregate network utility (line 7). Assuming a resource of one unit<sup>11</sup> in each of the contention regions, the chosen link ( $c$ ) obtains its proportional fair allocation of  $\min(\frac{\min\_resource_1}{\text{potential degree}}, \min\_resource_2)$  (line 8), where

$$\begin{aligned} \min\_resource_1 &= \min\{resource_c\}, \\ &\text{where } c \in \{UM(i), i \in P_j\} \\ \min\_resource_2 &= \min\{resource_d\}, \text{ where } d \in M(j). \end{aligned}$$

11. Based on the number of elements, the resources in a contention region and, hence, the solution can be directly scaled by the number of elements.

10. Fig. 6a can also be used as a reference.

Hence,  $min\_resource_1$  corresponds to the minimum of the resources left in the contention regions of  $j$  in which there exists a link to exploit its sacrificed utility.  $min\_resource_2$ , on the other hand, corresponds to the minimum of the resources left in all of the contention regions of  $j$ . Link  $c$ , being the highest ranked link in our example, obtains an allocation of  $min(\frac{1}{6}, 1) = \frac{1}{6}$ . Having allocated rate to the chosen link  $j$  (link  $c$ ), the resources in the contention regions that  $j$  belongs to are updated to reflect the remaining resources (line 9). Link  $j$  is then removed from the set RED and the rest of the red links are reranked without taking  $j$  into consideration, using the same procedure described above (line 10). Once again, the newly highest ranked red link is chosen and allocated its proportional fair share as before. However, when two red links have the same rank, then the red link that would obtain a lower rate is allocated first. This would create more potential for the remaining lower ranked red links and white links to exploit the sacrificed utility, thereby resulting in higher aggregate utility. The process of reranking and allocation iterates until all red links have obtained their respective proportional fair shares. In our example, after allocation to link  $c$ , link  $d$  obtains the highest rank and an allocation of  $min(\frac{5}{6}, \frac{1}{3}, \frac{5}{6}) = \frac{5}{18}$ , followed by link  $a$  with an allocation of

$$min\left(\frac{5}{6}, \frac{1}{2}, \frac{2}{3}, \frac{5}{6}\right) = \frac{5}{12}.$$

Finally, the white links in every contention region share the remaining resources in the contention region equally (line 11). Thus, links  $b$ ,  $e$ , and  $f$  obtain an allocation of  $\frac{5}{12}$ ,  $\frac{5}{18}$  and  $\frac{5}{18}$ , respectively. The final proportional fair allocation vector for our example is  $\{\frac{5}{12}, \frac{5}{12}, \frac{1}{6}, \frac{5}{18}, \frac{5}{18}, \frac{5}{18}\}$ . The main components responsible for obtaining a proportional fair allocation are ranking and the allocation based on the potential degree. Another possible method to obtain the proportional fair allocation is to begin with a max-min allocation. Then, starting with the flow having the largest potential degree, find the reduction in its allocation that would result in the maximum aggregate network utility and iterate thereafter for the remaining flows [23]. This would result in the same allocation vector as well.

#### 4.2.4 Scheduling

Once the proportional fair allocation has been obtained, the next step is to obtain a schedule that would achieve the corresponding rate allocation (Step 4). Further, in the process of scheduling, we also need to incorporate the optimization considerations. The minimum number of slot<sup>12</sup>-scheduling required to achieve a proportional fair integer allocation is given by the least common integer  $L$  that results in an integral slot allocation for all the links (line 12). In our example,  $L = 36$  time slots. Every link  $i$  has to be scheduled for  $l_i = (s_i \cdot L)$  slots within the span of  $L$  slots (line 13). The schedule is obtained as a two-level scheduling of the red links followed by the white links.

A red (bottleneck) link can be scheduled in any slot only if it can operate on all  $K$  (= number of elements) streams. Before a link is scheduled, both its neighbors and itself are checked for availability of sufficient resources for the upcoming transmission (lines 24 and 26). For this purpose,

every link  $i$  maintains a resource variable  $res_i$  reflecting the amount of resources remaining at the link in every slot. This variable gets updated on every transmission by a link  $k$  in its contention region and the strength of the interference caused by the transmission  $w_{ik}$  is also taken into account, thereby helping leverage the flexible interference suppression capability (lines 17 and 20). The red link (say  $j$ ) with the highest rank is scheduled first for  $l_j$  slots (line 25). During each slot of its schedule, the algorithm also attempts to maximize the utilization, i.e., after scheduling the highest ranked red link, the algorithm checks to see if any other red links (in the order of their ranks) that need allocation can be scheduled in the same slot with  $K$  streams (line 15). All such red links are scheduled in the same slot. In addition to these red links, all the white links that can be allocated at least one stream in that slot are also scheduled (lines 16-19). Then, the algorithm attempts to increase the number of streams that these scheduled white links can obtain in the same slot (lines 18-20). Note that, while the red links can be scheduled only if they can obtain  $K$  streams, the white links can be scheduled even if they can obtain one stream. But, among the white links that can be scheduled, the algorithm performs a fair allocation of streams (stream control). The scheduling of white links in the same slot as that of red links (if possible) exploits spatial reuse and thereby helps maximize utilization. After the schedule of a link in a slot, the algorithm keeps track of the remaining number of slots (streams) that the link needs to be allocated (lines 16 and 19). Once the highest ranked red link has been scheduled its share of slots, the algorithm checks the red link with the next rank for its share of slots (streams) that still remain to be allocated and the above procedure repeats (line 15).

Once all the red links have obtained their respective allocation of slots, the algorithm moves to schedule the white links (line 18). All the white links that still require allocation of slots to achieve their fair share can be scheduled in parallel in each slot thereafter till each one of them achieves its respective fair share. The allocation is done on a stream by stream basis to the white links (lines 19-20). Thus, the white links within a contention region (say  $w$  in number) share the  $K$  streams as  $\frac{K}{w}$  in each slot to get scheduled in parallel for  $l_i \cdot w$  slots, thereby performing stream control. Further, the white links, by virtue of performing stream control, can leverage the flexible interference suppression capabilities to increase the fair share in their contention region. Finally, by allowing only the nonbottleneck (white) links to perform stream control, we also eliminate the passive receiver overloading problem and the consequent degradation in network utilization.

In the example considered, red link  $c$  will get scheduled first for six slots operating on all  $K$  streams. However, no other link can be scheduled along with it. Red link  $d$  is then scheduled for 10 slots from slots 7-16 on all  $K$  streams. During the schedule of  $d$ , white link  $b$  can also be scheduled in parallel for the 10 slots. Since there are no other white links in its contention region, it gets scheduled with all  $K$  streams. The last red link ( $a$ ) is scheduled for 15 slots from slot 17-31 with all  $K$  streams. During its schedule, white links  $e$  and  $f$  are also scheduled for the 15 slots operating on  $\frac{K}{2}$  stream each, thereby performing stream control. Finally, from slots 32-36, white links  $b$ ,  $e$ , and  $f$  obtain their remaining share of allocation for five slots, with  $e$  and  $f$  performing stream control as before. Thus, at the end of 36 slots, every link obtains its share of allocation to result

12. Slot corresponds to the time for a packet transmission in the centralized approach.

in a proportionally fair allocation. The entire schedule then repeats all over again.

## 5 DISTRIBUTED SCMA

In this section, we present the distributed SCMA MAC scheme that aims to approximate the centralized algorithm. The distributed scheme achieves this goal in a purely localized manner without the requirement of any large-scale coordination in the network. We first identify the key challenges involved in realizing the centralized algorithm in a distributed fashion. Then, we use design elements and mechanisms that address these key challenges as building blocks and present the distributed algorithm. Finally, we describe the details of the distributed mechanisms, concluding the section with some practical considerations. For convenience, we shall refer to the distributed SCMA scheme as simply the SCMA scheme and the centralized SCMA scheme as simply the centralized scheme in the rest of the paper.

### 5.1 Overview

The basic components inherent in the design of SCMA are outlined below:

- The SCMA MAC scheme is a variant of CSMA/CA. Though CSMA/CA is widely deployed over ad hoc networks with omnidirectional antennas, its two key elements, namely, *carrier sensing* and *collision avoidance*, are still necessary for the target environment employing MIMO, although for a slightly different purpose. While carrier sensing in the omnidirectional environment refers to a node sensing the state of the channel, thereby deciding whether to transmit or not, its significance is greater in the case of a MIMO environment. The node has to sense the channel in order to determine the number of resources (streams) that it has to sacrifice to suppress the interference and, consequently, determine the remaining resources that can be used for transmission. Collision avoidance for the MIMO environment has a similar significance. The transmitter is unaware of the channel state around its receiver and other neighbors, which in turn necessitates the exchange of control information between the nodes. Although the motivation for collision avoidance is the same as in the omnidirectional environment, the purpose is to obtain information of available resources at the receiver, and other neighbors, and thereby make a decision on the number of resources to be used for transmission.
- Although SCMA performs collision avoidance, the contention resolution no longer happens in the backoff domain. Instead, SCMA performs contention resolution in the persistence domain similar to [20], which makes it easier to achieve a proportional fairness model. Further, it has been shown in [20] that, if the persistence parameters ( $x_i$ ) of the flows are adapted according to

$$\dot{x}_i = \alpha - \beta p_i x_i, \quad (8)$$

then the system converges to the optimal point of maximizing the aggregate network utilization for a proportional fairness model.  $\alpha$  and  $\beta$  are system parameters,  $p_i$  is the loss probability experienced by

the flow, and  $\dot{x}_i$  is the rate of change of persistence. Hence, if the persistence parameter is assumed to be indicative of the rate experienced by the flow, (8) suggests that, by performing a linear increase proportional decrease (LIPD) adaptation of the rate, one can achieve proportional fairness. Proportional decrease in this context refers to a decrease of rate that is proportional to the loss experienced by the flow, which in turn is dependent on the number of contention regions it belongs to as well as the number of flows within each of those contention regions.

- However, the above adaptation assumes a single-level scheduling. Hence, to extend the adaptation to the dual scheduling (red and white links) employed in SCMA, the persistence value ( $P_{old}$ ) obtained from the basic adaptation is translated into a new persistence value,  $P_{new}$ . This  $P_{new}$  is the same as that of  $P_{old}$  for the red links, while it is scaled up for the white links. Since the white links in a clique operate simultaneously, using only a subset of the streams ( $K_{new} \leq K_{old} = k$ ), their  $P_{new}$  value will be a scaled version of  $P_{old}$  as in

$$P_{new} = (P_{old} * K_{old}) / K_{new}. \quad (9)$$

The entire adaptation process still happens on the  $P_{old}$  values, but the links thereafter appropriately identify their  $P_{new}$  value based on their color and use it to determine access to the channel. This ensures that the resulting channel allocation vector is still a proportionally fair one. Further details on the adaptation mechanism are provided in Section 5.3.2.

### 5.2 Challenges

The key challenges in realizing the centralized algorithm in a distributed manner are:

- *Coloring.* While it is relatively easy to color the links in the centralized algorithm, it is a nontrivial task to detect the number of cliques that each link belongs to and color accordingly in a purely distributed fashion. Briefly, in SCMA, a node observes the number of streams transmitted during each slot in its vicinity between the two successive slots through which it gets access to the channel. If the node perceives more than  $k$  ( $k$  being the number of antenna elements) streams during any of the slots, it colors itself red. Otherwise, it colors itself white.
- *Fair Allocation.* We adopt a proportional fairness model similar to the one used in PFCR [20] for SCMA, where the utility function is represented as  $U(x) = \log(x)$  with  $x$  referring to the channel allocation. In SCMA, due to the distinction necessary between red links and white links, the channel access mechanism for the white links (involving stream control) is different from that of the red links. Hence, the adaptation of the persistence parameter for the white links must be appropriately tuned such that proportional fairness is still ensured.
- *Stream Control.* Once the nodes have identified the color of the links that they belong to, it now becomes crucial for the transmitting nodes of the white links to estimate the fair share in order to perform stream control in their contention region (clique). While an overestimate of the fair share could result in a

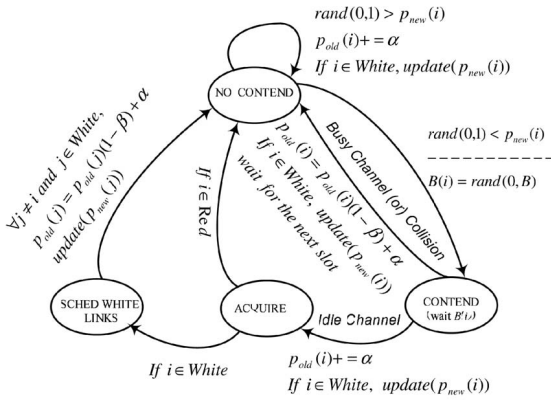


Fig. 8. SCMA State Diagram.

collision in several of the clique members and could hence be detrimental, an underestimate could result in potential underutilization. Furthermore, in the presence of network dynamics where new white links join the clique or existing white links leave the clique, the resulting transmitters of the white links should then be able to converge to the new fair share in the clique in a short time. The transmitters of the white links in a contention region individually perform adaptation to keep track of their fair share of resources in the clique. Also, they perform a form of coordinated scheduling with other white links belonging to the same clique to maximize utilization. We will elaborate on these mechanisms later in this section.

### 5.3 Distributed Algorithm

We now present the components of the distributed algorithm that address these challenges in the process of approximating the centralized algorithm. In addition, the design of these components also helps leverage the advantages provided by the optimization considerations. The state diagram and the pseudocode for the algorithm are presented in Figs. 8 and 9, respectively.

#### 5.3.1 Coloring

Coloring is necessary to distinguish between the red and white links in order to leverage the optimization considerations. It is sufficient if the links are able to identify whether they belong to multiple contention regions or not, instead of actually identifying the number of contention regions they belong to, for the process of coloring. Further, only a red link will be overwhelmed in terms of resources due to members of the different cliques that it belongs to, transmitting at the same time. This fact is exploited in aiding the transmitting and receiving nodes in determining the color of their respective links.

Every transmitter initially starts transmitting on all the streams (with  $P_{new} = P_{old}$ ) like CSMA/CA(k) until it determines its color. It locally determines the color of its link in conjunction with its receiver. Specifically, the transmitter observes the usage of resources between every two slots that it has gained access to the channel. If the transmitter or the receiver observes more than  $k$  streams during any of the slots<sup>13</sup> that it has not obtained access to

13. Slot corresponds to the duration of an RTS/CTS/DATA/ACK exchange in the distributed approach.

```

CONTEND()
1  $\forall$  Slot  $S$ , node  $i$ 
2 state = NO_CONTENT
3 If  $uniform(0, 1) \leq P_{new,i}$ 
4 state = CONTENT
5  $B_i = uniform(0, B)$ 
6 Defer( $B_i$ )
7 If ( $Check\_resources() == Available$ )
8 Acquire_channel()
9 If ( $Acquire\_status() == Collision$ )
10  $P_{old,i} = P_{old,i} * (1 - \beta)$ 
11 If  $i \in WHITE$ 
12  $P_{new,i} = \frac{P_{old,i} * K_{old,i}}{K_{new,i}}$ 
13 else state = ACQUIRE
14  $\forall j \in Neighbor(i)$ 
15 Update Resources
16 If ( $resources_j < 0$ ),  $color(j) = RED$ 
17 Recolor( $i$ )
18 If ( $i \in WHITE$ ), Co-ordinate_Schedule( $i$ )
19 If ( $Remaining\_resources(i)$ )
20  $K_{new,i} = K_{new,i} + \frac{Remaining\_resources(i)}{white\_count}$ 
21 else  $P_{old,i} = P_{old,i} * (1 - \beta)$ 
22 If  $i \in WHITE$ 
23  $P_{new,i} = \frac{P_{old,i} * K_{old,i}}{K_{new,i}}$ 
24  $P_{old,i} = P_{old,i} + \alpha$ 
25 If  $i \in WHITE$ 
26  $P_{new,i} = \frac{P_{old,i} * K_{old,i}}{K_{new,i}}$ 

Co-ordinated_Schedule( $i$ )
27  $\forall j \in Neighbor(i) \ \&\& \ color(j) == WHITE$ 
28  $P_{old,j} = P_{old,j} * (1 - \beta)$ 
29  $P_{new,j} = \frac{P_{old,j} * K_{old,j}}{K_{new,j}}$ 
Recolor( $i$ )
30 Check slot history from previous service slot
in conjunction with receiver to color
31 If  $i \in WHITE$ ,  $K_{new,i} = \frac{K_{old,i}}{white\_count}$ 

```

Fig. 9. Pseudocode for the distributed algorithm.

the channel, then the link is automatically colored red (line 16). It is possible for a link to be red even if the transmitter and the receiver individually do not observe more than  $k$  streams. This is because there could be an active link within the interference range of the transmitter, but not within that of the receiver or vice versa. The transmitter and receiver in this case would not be able to “independently” identify the correct color. Hence, the transmitter, during its RTS/CTS exchanges with the receiver, compares its version of the winner list (IDs of nodes that have obtained channel access in its neighborhood) with that of the receiver for the slots in between their successive channel accesses. If the list happens to be different in at least one of the slots, then the link is colored red since this effectively means that this link as a whole is exposed to more than  $k$  stream transmissions at the same time (line 17). Otherwise, the link is colored white.

#### 5.3.2 Contention and Channel Access

Once the nodes have successfully colored their respective links, they adopt a channel contention mechanism that is tuned to their color. There are four possible states in which a node can be, namely, *Contend*, *No\_Contend*, *Acquire*, and *Sched\_White\_Links* (Fig. 8). Every node having a packet to transmit first decides to contend for the channel with a probability of  $P_{new}$ . This persistence probability  $P_{new}$  is the same as  $P_{old}$  for the red links, while it is scaled for the white links (line 12). If the node succeeds, it moves from the *No\_Contend* state to the *Contend* state (lines 2-4), where it chooses a waiting time uniformly distributed from the interval  $(0, B)$ .  $B$  is a constant and set to 32 in the simulations, as advocated in [20]. The node then waits for

the backoff period (in slots), after which it tries to access the channel to see if the channel is busy (lines 5-7). The busy state of the channel in our case corresponds to a lack of sufficient amount of resources at the transmitter or the receiver or the two-hop neighbors.

If the node finds the channel to be busy, it gives up the slot and decrements its persistence by  $\beta * P_{old}$ . Similarly, if the channel is idle but if the node faces or detects collision, it decrements its persistence by a factor of  $\beta$ . In addition to decrementing the value of  $P_{old}$ , if the node belongs to a white link, then it also has to update its  $P_{new}$  value (lines 8-12). On the other hand, if the node finds the channel to be idle and does not experience any collision, then it moves to the *Acquire* state, where it transmits. Every node in the two-hop neighborhood of this transmission would automatically expend the appropriate number of resources to suppress this transmission (line 15). At the end of the slot, all the nodes having a packet to transmit in the next slot increase their persistence  $P_{old}$  by  $\alpha$ , with the white links also updating their  $P_{new}$  value (lines 24-26). The values of  $\alpha$  and  $\beta$  are chosen to be 0.1 and 0.5 based on the rationale provided in [20].

In being able to determine if the channel is busy, a node needs to know about the resource availability at nodes in its two hop neighborhood. This can be achieved by piggybacking the amount of resources remaining at a node in its control packet transmissions. However, to make these control packets decodeable in the two-hop neighborhood, the reception range needs to be extended by a factor of two. This in turn can be achieved by transmitting the control (RTS/CTS) packets as multiple copies (dependent signals) on at least four streams (using space-time block codes). In this case, we exploit the diversity gain of MIMO to provide us with this range extension factor of two (with four element DAAs and a path loss exponent of 4), instead of its spatial multiplexing gain. Note that this range extension will not be the same in all directions and will depend on the radiation pattern currently used by the transmitting node. This range extension mechanism has the additional benefit of aiding the white links in their stream control process, which we explain subsequently. One might think that the disadvantage of not performing spatial multiplexing for the control packets might lead to a degradation in performance. But, our contention is that the benefits of diversity gain for control packets is much more significant in terms of addressing several of the issues associated with distributed operations.

### 5.3.3 White Link Adaptation

For the white links to be able to perform stream control and, hence, determine the appropriate persistence ( $P_{new}$ ) with which to contend for the channel, they need to estimate the fair share of resources to use in their contention region. While the computation of fair share of the red links is relatively easy ( $k$  streams), the fair share estimation for the white links is nontrivial.

Every node advertises the color of its link (if colored) in its transmissions. During the initial phase, when a white link may not be aware of the other white links in its contention region, it will not be able to arrive at the correct fair share. Hence for this purpose, every node transmits for one more slot on all  $k$  streams (even after it has colored itself white) along with its color information to inform the other members of the clique about its newly colored link. Since the control packets are decodeable within a range that is twice the normal reception range due to the diversity gain,

the other members of the clique will receive this information. This helps the white links keep track of the number of white links in the same clique (say  $w$ ) and, hence, help them arrive at the fair share in the clique  $k_{new} (= \frac{k}{w})$  (line 31).

### 5.3.4 Coordinated Scheduling

Distributed execution of the stream control mechanism by the white links is a challenge that has to be accomplished. This requires that the white links operate simultaneously on a subset of the maximum allowable number of streams. Since persistence is used to ensure proportional fairness, it is possible that only some of the white links in a clique actually contend for a slot. Hence, even if one of the white links gains access to the channel, it must be ensured that all the other white links in the same clique are also scheduled in the same slot, failing which the advantage of stream control cannot be leveraged.

Accordingly, when the first white link in a clique gains access to the channel, it also coordinates the other white links in the clique to transmit in that slot using their own estimated fair share (line 18). This corresponds to the node entering the *Sched\_White\_Links* state in Fig. 8. Specifically, this link's RTS/CTS messages will contain a flag ordering the schedule of all the white links in the clique. Since the control messages can be decoded within the two-hop neighborhood (owing to the range extension factor of two), all the white links in the clique will be able to listen to the command of this initiating link and thereby schedule themselves in the same slot, irrespective of whether they contended for channel access in that slot or not. However, the contending white links that were not the initiator of the coordinated scheduling will still have their  $P_{old}$  values decremented by the factor  $\beta$  to be in conformance with the normal adaptation algorithm (lines 27-29).

In addition, to be able to leverage the advantages of flexible interference suppression, the nodes belonging to white links observe if their fair share can be increased based on the remaining resources available at the end of their transmission (line 20). If so, the node increases its fair share only by a fraction of the remaining resources to allow other white links in the clique to increase their fair share as well. Thus, the resources are fully utilized in the clique, thereby leveraging the advantage of flexible interference suppression.

## 6 PERFORMANCE EVALUATION

In this section, we present performance results for SCMA obtained through simulation studies. We use an event-driven packet level simulator for recording the results. We use UDP as the transport layer protocol and CBR as the traffic generator. The packets are generated at a rate of 100 packets/sec and are of size 1Kbyte. The number of flows and elements in the antenna array are parameters that vary from one experiment to another. We extend the distributed proportional fair contention resolution (PFCR) mechanism [20] to PFCR( $k$ ) and CSMA/CA to CSMA/CA( $k$ ) for ad hoc networks with MIMO links and consider these as baseline protocols in our simulation study. CSMA/CA( $k$ ) and PFCR( $k$ ) are variants of CSMA/CA and PFCR, respectively, that use  $k$  streams for their transmissions and receptions. Further, we use a simple model that conservatively<sup>14</sup> assumes only about 20 percent gain from performing stream

14. The statistical gains on the different streams could have significant disparities resulting in a much larger gain [16].

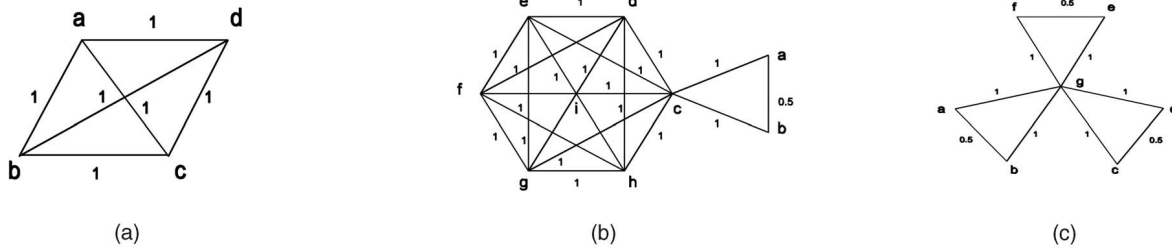


Fig. 10. Flow contention topologies. (a) Scenario 1, (b) Scenario 2, and (c) Scenario 3.

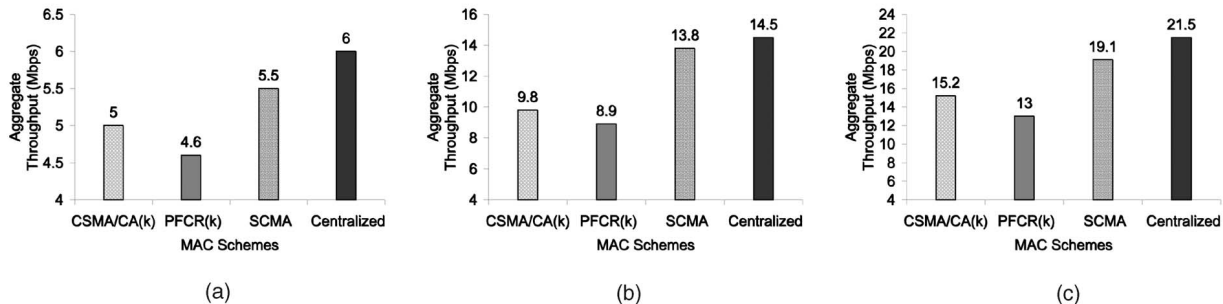


Fig. 11. Throughput. (a) Scenario 1, (b) Scenario 2, and (c) Scenario 3.

control. We compare the performance of SCMA, CSMA/CA(k), and PFCR(k) with that of the centralized protocol and thereby present results to highlight the benefits of the mechanisms involved in our distributed protocol. The metrics we use for comparing the various schemes are *throughput* and *relative standard deviation*. Since the algorithm provides proportional fairness that is location dependent, standard deviation or normalized standard deviation would not be able to capture well the degree of fairness provided by the scheme. Hence, we have chosen to use relative standard deviation as the fairness metric. Specifically, the distribution of throughput of the various schemes is compared against that of the centralized scheme and the deviation normalized to the mean is obtained.

## 6.1 Macroscopic Results

We now present a set of representative topologies to highlight the advantages of stream control and flexible resource usage.

### 6.1.1 Toy Topologies

We discuss the results with respect to the throughput metric first, followed by the fairness metric:

- *Scenario 1*. This scenario is used to highlight the gains from performing pure stream control. We consider a simple four-clique flow contention graph, as shown in Fig. 10a. Each node has a four-element DAA. The comparative results for the different schemes are presented in Fig. 11a. All the links are white in this case and, since all the link weights are 1, there is no performance gain due to flexible interference suppression. The gain of SCMA over PFCR(k) and CSMA/CA(k) (10-20 percent) is solely contributed by stream control since each link in the clique transmits in every slot on a single stream. Further, CSMA/CA(k) performs better than PFCR(k). But, as we shall show later,

the degree of fairness provided by PFCR(k) is much higher than that of CSMA/CA(k).

- *Scenario 2*. This scenario is used to highlight the gains from performing both stream control and flexible interference suppression, with stream control being the dominating contributor. We consider a flow contention topology made up of both red and white links as shown in Fig. 10b. The link  $c$  belongs to two cliques and is the only red link in this topology. Every node in the network has an array of five elements. The edge weight between the white links  $a$  and  $b$  is 0.5. This indicates that the links  $a$  and  $b$  can potentially use twice their fair share in the clique since they will require sacrificing only one stream for every two streams used by the other white link. The result in Fig. 11b indicates that SCMA achieves a net gain of about 40 percent over PFCR(k) of which about 15 percent is contributed solely by the additional resources made available at the links  $b$  and  $a$  due to flexible interference suppression. Since we have a clique of size six of which five links are white, this represents the case of maximum stream control gain that can be achieved with five elements. All of the five links operate simultaneously on a single stream each to provide a gain of about 25 percent.
- *Scenario 3*. This scenario is also used to highlight the gains from performing both stream control and flexible interference suppression, but with flexible interference suppression being the dominating contributor. In Fig. 10c, we consider a single red link that is a part of three cliques. Every node has an array of six elements each. To highlight the significant improvement that can be obtained by performing flexible interference suppression, we consider three sets of weakly interfering links with edge weights of 0.5 each. The result in Fig. 11c indicates that SCMA achieves a gain of about 46 percent of which a significant portion of around

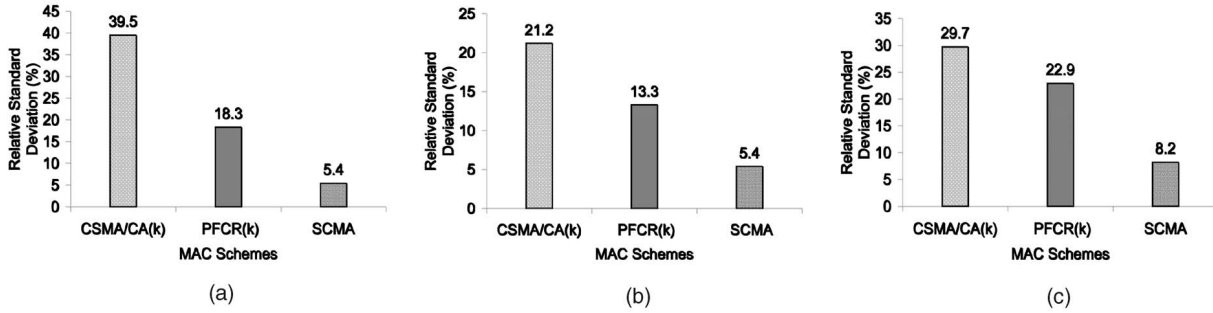


Fig. 12. Unfairness (%). (a) Scenario 1, (b) Scenario 2, and (c) Scenario 3.

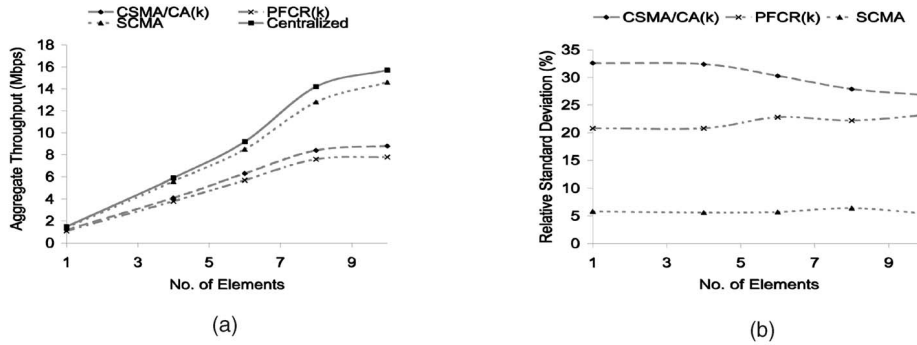


Fig. 13. Typical network topologies. (a) Throughput and (b) unfairness.

30 percent is contributed purely by the additional resources made available at the outer links of the topology. Though the outer links have a six-element DAA, they end up using only three streams since the cliques are all of size three with two white links in each. Hence, the maximum gain of stream control for a six element case (when six links use one stream each) cannot be obtained in this case. However, note that CSMA/CA(k) or PFCR(k) cannot leverage the gain of flexible interference suppression because they do not perform stream control.

In terms of fairness, Fig. 12 presents the relative standard deviation for the representative topologies considered thus far. Since the centralized algorithm is ideally fair, we present the relative standard deviation of the throughput distributions obtained by the various schemes with respect to the centralized scheme. It can be observed that PFCR(k) reduces the degree of unfairness by more than 50 percent as compared to CSMA/CA(k). Moreover, SCMA further provides a better degree of fairness over PFCR(k) by more than 50 percent. This could be attributed to the fact that SCMA, by virtue of performing stream control, is able to allocate streams to the links on a much finer granularity than CSMA/CA(k) or PFCR(k) wherein the granularity of stream allocation is always  $k$  streams.

### 6.1.2 Typical Network Topologies

For more generic topologies, we consider a random network topology consisting of 50 nodes distributed uniformly over an area of 750m by 750m. The random scenarios are generated using the *setdest* tool and the results are averaged over several seeds and also across a different number of elements present in the antenna array. Mobility is not considered in these scenarios. Figs. 13a and 13b present the results for the various schemes in comparison with the centralized scheme. The utilization in Fig. 13a

shows an increasing trend with the number of elements for all the schemes. However, for CSMA/CA(k) and PFCR(k), the improvement in utilization obtained for every extra element employed starts to decrease due to the absence of stream control. Hence, the scalability of SCMA in terms of utilization is better when compared to CSMA/CA(k) and PFCR(k). The fairness results are presented in Fig. 13b. Although we are not able to conclude any relation about the trend in fairness with respect to the number of elements, the result clearly shows that SCMA provides an improvement of around 15 percent to 25 percent when compared to CSMA/CA(k) and PFCR(k).

## 6.2 Microscopic Results

- Convergence of Coloring.** In order to leverage the advantage of stream control effectively, a node must first color its link correctly. Hence, we investigate the efficiency of the coloring mechanism employed by SCMA. We consider the topology shown in Fig. 10b for this purpose. The topology consists of one red link and seven white links. The result presented in Fig. 14a indicates the amount of time it takes for SCMA to complete the coloring. The x-axis is measured in slot sequences, where each slot sequence corresponds on an average to the time taken for all the members of the largest clique to get access to the channel once. Note that every link takes at least two slot sequences in SCMA to color itself and accordingly start using the appropriate number of streams. Hence, we measure the convergence time in terms of slot sequences. The result shows that the coloring done by SCMA converges to that of the centralized scheme in only about three to four slot sequences.
- Convergence to Fair Share—Network Dynamics.** The second important aspect of the distributed mechanism after coloring is to ensure that the

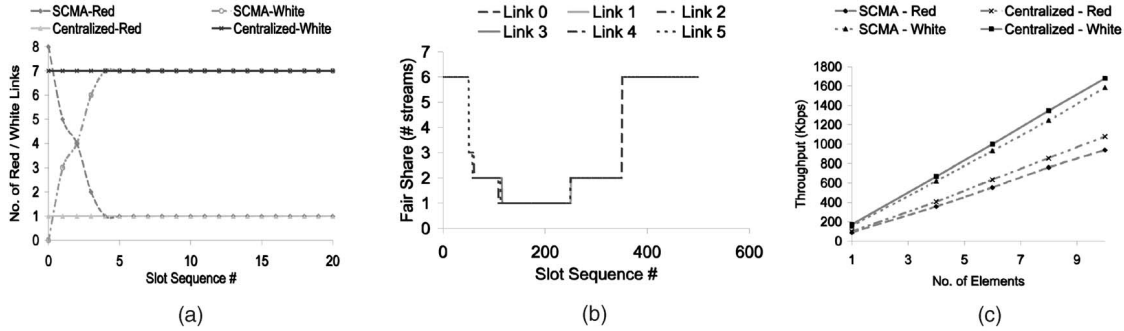


Fig. 14. Microscopic results. (a) Coloring convergence (slot sequences), (b) fair share convergence (slots), and (c) throughput (red/white).

colored links use the appropriate number of streams. This is not a problem for the red links, which operate on all the streams. Hence, we study the impact of dynamics in the network on the estimation of fair share by the white links. We consider the dynamic topology of a single clique whose clique size basically varies with time as new links come in and existing links leave the clique. All the nodes possess a six element DAA each. The result is presented in Fig. 14b. Essentially, the topology is created as a single-link clique, builds to a three-link clique at the end of 50 slots, and, finally, to a six-link clique at the end of 100 slots. The single link initially operates on all six streams. With the entry of two more links at the 50th slot, the fair share converges to two streams within five slots. Then, with the entry of three more links at the 100th slot, the fair share further reduces and converges to one stream within about 10 to 15 slots ( $<$  three slot sequences). We also consider the case of existing links leaving the clique wherein three flows (links) leave at the end of 250 slots and two more at the end of 350 slots. In both these cases, the remaining links are able to utilize the resources left over by the departing links almost instantaneously. Although time is measured directly in terms of slots here, as opposed to slot sequences, we can easily translate the result for slot sequences. Note that the convergence in the case of white links leaving the clique happens much faster than the case of new white links coming in. This is because, when new white links come in, they first color themselves before estimating their fair share and the existing white links in the clique then converge to this new fair share. On the other hand, when white links leave the clique, the remaining white links locally estimate the new fair share in the clique, based on the free resources remaining at the nodes after accounting for the transmissions in the clique, without the need for any coloring.

- *Red-White Deviation.* Earlier in the section we presented aggregate throughput results for the random scenarios. We now present the throughput obtained by the red and white links in SCMA, averaged across the seeds and compare it with that of the centralized algorithm. This is to ensure that SCMA provides a fair distribution of throughput not just on an aggregate basis but also individually

with respect to the red and white links. This is captured in Fig. 14c. It can be seen that the throughput obtained by the red and white links in SCMA are close enough to those obtained in the centralized algorithm.

## 7 RELATED WORK

To the best of our knowledge, we are not aware of any existing MAC protocols for ad hoc networks with MIMO links in the literature. However, there has been significant contribution in the related area of directional (switched beam) antennas. Hence, we provide a short synopsis of the related work in the area of MAC protocol for ad hoc networks with directional antennas.

Shad et al. [24] consider a cellular scenario in which the base-station is equipped with a multibeamforming antenna, and discusses the improvement in static SDMA/TDMA system capacity on performing dynamic slot assignment. However, the scope of the work does not include ad hoc networks. References [10], [11], [25], [26], [27] propose MAC protocols for ad hoc networks with directional (switched beam) antennas. While directional antennas offer more spatial flexibility when compared to omnidirectional antennas, they are more restrictive than the MIMO links we consider in this paper. Choudhury et al. [10] and Nasipuri et al. [28] use the directive gain provided by directional antennas for the purpose of range extension and minimization of power consumption, respectively. However, the focus is not on MIMO links. Nandagopal et al. [20] presents the proportional fairness model for the problem of channel allocation in wireless ad hoc networks, which we have augmented with several design optimizations that are specific to the MIMO environment. Finally, Krishnamurthy et al. [29] present a polling-based media access protocol for the environment of cellular networks with smart antennas being employed at the base stations. But, the scheme cannot be extended to work for ad hoc networks due to its centralized nature.

## 8 CONCLUSIONS

We have identified the potential advantages of MIMO links in wireless ad hoc networks. The problem of fair channel allocation for the target environment has been presented and the key optimization considerations for the design of an ideal MAC protocol for such an environment have been discussed. We have presented a centralized algorithm that incorporates the propitious characteristics of MIMO links as well as the optimizations possible in relation to MIMO environments. We have also proposed a distributed MAC protocol, called the SCMA, that approximates the centralized version. The proposed SCMA scheme clearly outperforms CSMA/CA(k)

and PFCR(k) protocols and performs nearly as well as the centralized algorithm, suggesting that it is beneficial to employ SCMA as the MAC layer protocol for MIMO environments. We are also currently investigating the possibility of moving the contention resolution mechanism of SCMA to the backoff domain.

## APPENDIX

### PERFORMANCE BOUNDS

While spatial multiplexing can help increase the capacity of the link directly, diversity gain, which provides an increase in the SNR of the link for a fixed error probability requirement, can be used indirectly for power consumption minimization or increasing the communication range of the link. Since power control can itself be considered as an independent direction of optimization, we do not consider power control in this work. The focus here is to explore the trade offs of exploiting spatial multiplexing for increasing capacity (rate) versus diversity for increasing range in ad hoc networks.

The model assumed for this analysis is similar to the one used in [30]. Let us consider a random network as a unit area disc with  $n$  nodes, each capable of generating  $\lambda(n)$  bits/sec of traffic to a random destination. Let the bandwidth of the wireless channel be  $W$ . From the seminal work in [30], we know that the per node throughput is of the order of

$$O\left(\frac{W}{\sqrt{n \log n}}\right).$$

More specifically, when edge effects are incorporated, the following inequality holds:

$$n\lambda(n)\bar{h} \leq \frac{16W}{\pi\Delta^2 r^2}, \quad (10)$$

where  $\bar{h}$  represents the average hop count and  $r$  the transmission/reception range.  $\Delta$  represents the guard zone parameter which roughly determines the region silenced by a transmission and is, hence, dependent on the physical layer technology and the MAC protocol employed. When the radius of transmission is increased, the hop length and, hence, the multihop burden is decreased. However, the spatial reuse also decreases. The decrease in spatial reuse is more than the decrease in hop length. Hence, it has been argued in [30] that the maximum throughput can be obtained only when the radius of transmission is maintained as small as possible so as to just ensure connectivity. This critical radius is given by

$$r = \sqrt{\frac{\log n}{\pi n}}$$

and, at this critical radius, the bound on the throughput has been obtained to be  $O\left(\frac{W}{\sqrt{n \log n}}\right)$ .

At a high level, it can be observed that there are three components that determine the scaling nature of the throughput in (10), 1) number of nodes, 2) number of simultaneous transmissions (or) spatial reuse, and 3) average hop length  $\bar{h}$ . The number of nodes and the hop length determine the impact caused by the multihop nature of the flows and, hence, have a negative influence on the throughput. The number of simultaneous transmissions, on the other hand, has a positive influence on throughput and is made possible due to the limited transmission ranges employed. However, the degree of spatial reuse will be dependent on the radius of transmission as well as the

guard zone used by the MAC protocol. When the edge effects are considered, the spatial reuse has been shown to be bounded by

$$\frac{16A}{\pi\Delta^2 r^2},$$

where  $A$  is the area of the network.

In the case of MIMO links, spatial multiplexing can increase the capacity of the link by a factor that is linear in the number of antennas elements employed. This factor is given by the minimum of the transmitter and receiver antenna elements. This increased capacity of the links can directly be translated to a linear increase in the network and per-node throughput as well. In effect, the spatial reuse in (10) can be visualized to be scaled by a linear factor that is given by the minimum of the transmitter and receiver antenna elements. The linear increase in throughput can now be captured by the following inequality:

$$\lambda(n) \leq \frac{16W \cdot \min(M, N)}{\pi n \bar{h} \Delta^2 r^2}, \quad (11)$$

where  $M$  and  $N$  represent the number of antenna elements at the transmitter and receiver, respectively.

In the case of diversity, let us consider the case of diversity gain being exploited for range extension. If the function that characterizes the range increase is represented by  $f(P_e, d)$ <sup>15</sup> (where  $P_e$  denotes link error probability,  $d$  denotes diversity order =  $MN$ ), then, as the range of transmission increases from  $r$  to  $f \cdot r$ , the average hop length of routes decreases from  $\bar{h}$  by a factor of  $f$  to  $\frac{\bar{h}}{f}$ , while the inhibited zone due to a transmission is scaled up by a factor of  $f^2$ . Hence, the corresponding inequality becomes,

$$\lambda(n) \leq \frac{16W}{\frac{\pi n \bar{h}}{f \Delta^2 (r \cdot f)^2}} = \frac{16W}{\pi n \bar{h} \Delta^2 r^2 f}. \quad (12)$$

Thus, it can be easily seen from (11) and (12) that, while increasing rate through spatial multiplexing helps increase the per-node and, hence, aggregate throughput, increased range degrades system performance. This has motivated us to focus on spatial multiplexing from the perspective of increasing the aggregate network throughput in this work. However, note that this conclusion must not be generalized to other possible dimensions such as reliability, robustness, and energy efficiency, where the importance of diversity could be quite significant.

## ACKNOWLEDGMENTS

This work was funded in part by US National Science Foundation grants ITR-0313005 and ANI-0117840.

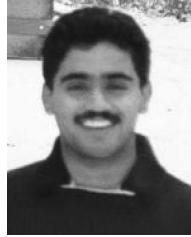
## REFERENCES

- [1] R.J. Mailloux, *Phased Array Antenna Handbook*. Artech House, 1993.
- [2] K-H. Li, M.A. Ingram, and E.O. Rausch, "Multibeam Antennas for Indoor Wireless Communications," *IEEE Trans. Comm.*, vol. 50, no. 2, pp. 192-194, Feb. 2002.
- [3] J.H. Winters and M.J. Gans, "The Range Increase of Adaptive versus Phased Arrays in Mobile Radio Systems," *IEEE Trans. Vehicular Technology*, vol. 48, no. 2, pp. 353-362, Mar. 1999.

15. At high SNR, this function can approximately be characterized from the relation,  $P_e \approx \frac{1}{SNR^d}$ .

- [4] D. Gesbert, M. Shafi, D. Shiu, P.J. Smith, and A. Naguib, "From Theory to Practice: An Overview of MIMO Space-Time Coded Wireless Systems," *IEEE J. Selected Areas in Comm.*, vol. 21, no. 3, pp. 281-301, Apr. 2003.
- [5] G.J. Foschini and M.J. Gans, "On Limits of Wireless Communications in a Fading Environment When Using Multiple Antennas," *Wireless Personal Comm.*, vol. 6, pp. 311-335, 1998.
- [6] G.J. Foschini, "Layered Space-Time Architecture for Wireless Communication," *Bell Labs Technical J.*, vol. 6, pp. 311-335, 1998.
- [7] J.C. Liberti and T.S. Rappaport, *Smart Antennas for Wireless Communications: IS-95 and Third Generation CDMA Applications*. Prentice Hall, 1999.
- [8] J.H. Winters, J. Salz, and R.D. Gitlin, "The Impact of Antenna Diversity on the Capacity of Wireless Communication Systems," *IEEE Trans. Comm.*, vol. 42, no. 2, 1994.
- [9] J.H. Winters, "Optimum Combining in Digital Mobile Radio with Cochannel Interference," *IEEE J. Selected Areas in Comm.*, vol. 2, pp. 528-539, July 1984.
- [10] R.R. Choudhury, X. Yang, R. Ramanathan, and N.H. Vaidya, "Using Directional Antennas for Medium Access Control in Ad Hoc Networks," *Proc. ACM MOBICOM*, Sept. 2002.
- [11] A. Nasipuri, S. Ye, and R.E. Hiromoto, "A MAC Protocol for Mobile Ad Hoc Networks Using Directional Antennas," *Proc. IEEE Wireless Comm. and Networking Conf.*, 2000.
- [12] J.B. Anderson, "Antenna Arrays in Mobile Communications: Gain, Diversity, and Channel Capacity," *IEEE Antennas and Propagation Magazine*, vol. 42, pp. 12-16, Apr. 2000.
- [13] L. Zheng and D. Tse, "Diversity and Multiplexing: A Fundamental Tradeoff in Multiple-Antenna Channels," *IEEE Trans. Information Theory*, vol. 49, no. 5, pp. 1073-1096, May 2003.
- [14] D. Shiu, G.J. Foschini, M.J. Gans, and J.M. Kahn, "Fading Correlation and Its Effect on the Capacity of Multiple-Element Antennas," *IEEE Trans. Comm.*, vol. 48, Mar. 2000.
- [15] S. Catreux, P.F. Driessen, and L.J. Greeststein, "Simulation Results for an Interference-Limited MIMO Cellular System," *IEEE Comm. Letters*, vol. 4, Nov. 2000.
- [16] M.F. Demirkol and M.A. Ingram, "Control Using Capacity Constraints for Interfering MIMO Links," *Proc. Int'l Symp. Personal, Indoor, and Mobile Radio Comm.*, vol. 3, pp. 1032-1036, Sept. 2002.
- [17] M.F. Demirkol and M.A. Ingram, "Stream Control in Networks with Interfering MIMO Links," *Proc. IEEE Wireless Comm. and Networking Conf.*, Mar. 2003.
- [18] A. Hottinen, R. Wichman, and O. Tirkkonen, *Multiantenna Transceiver Techniques for 3G and Beyond*. John Wiley and Sons, Feb. 2003.
- [19] J.-S. Jiang, M.F. Demirkol, and M.A. Ingram, "Measured Capacities at 5.8 GHz of Indoor MIMO Systems with MIMO Interference," *Proc. IEEE Fall Vehicular Technology Conf.*, Oct. 2003.
- [20] T. Nandagopal, T-E. Kim, X. Gao, and V. Bhargavan, "Achieving MAC Layer Fairness in Wireless Packet Networks," *Proc. ACM MOBICOM*, Aug. 2000.
- [21] D. Rose, R.E. Tarjan, and G. Lueker, "Algorithmic Aspects of Vertex Elimination on Graphs," *SIAM J.*, vol. 5, pp. 146-160, 1976.
- [22] D.R. Fulkerson and O.A. Gross, "Incidence Matrices and Interval Graphs," *Pacific J. Math.*, vol. 15, pp. 835-855, 1965.
- [23] D.M Chiu, "Some Observations on Fairness of Bandwidth Sharing," Sun Microsystems Technical Report, TR-99-80, Sept. 1999.
- [24] F. Shad, T. Todd, V. Kezys, and J. Litva, "Indoor SDMA Capacity Using a Smart Antenna Basestation," *Proc. IEEE Int'l Conf. Universal Personal Comm. (ICUPC)*, pp. 868-872, 1997.
- [25] Y.B. Ko, V. Shankarkumar, and N.H. Vaidya, "Medium Access Control Protocols Using Directional Antennas in Ad Hoc Networks," *Proc. IEEE INFOCOM*, Mar. 2000.
- [26] R. Ramanathan, "On the Performance of Ad Hoc Networks with Beamforming Antennas," *Proc. ACM MOBIHOC*, Oct. 2001.
- [27] M. Sanchez, T. Giles, and J. Zander, "CSMA/CA with Beam Forming Antennas in Multi-Hop Packet Radio Networks," *Proc. Swedish Workshop Wireless Ad Hoc Networks*, Mar. 2001.
- [28] A. Nasipuri, K. Li, and U.R. Sappidi, "Power Consumption and Throughput in Mobile Ad Hoc Networks Using Directional Antennas," *Proc. IEEE Int'l Conf. Computer Comm. and Networking (IC3N)*, Oct. 2002.
- [29] S. Krishnamurthy, A. Acampora, and M. Zorzi, "Polling Based Media Access Protocols for Use With Smart Adaptive Array Antennas," *IEEE Trans. Networking*, Apr. 2001.

- [30] P. Gupta and P.R. Kumar, "The Capacity of Wireless Networks," *IEEE Trans. Information Theory*, vol. 46, no. 2, pp. 388-404, Mar. 2000.



**Karthikeyan Sundaresan** received the bachelor's degree in electronics and communication engineering from Anna University in 2001. He joined the Electrical and Computer Engineering discipline at the Georgia Institute of Technology in 2001 where he received the master's degree in 2003. He is currently working toward the PhD degree at the same university. His research interests are in the field of wireless network protocols, wireless cross-layer protocol design and wireless multicarrier communications, and smart antennas. He is a student member of the IEEE.



**Raghupathy Sivakumar** received the master's and doctoral degrees in computer science from the University of Illinois at Urbana-Champaign in 1998 and 2000, respectively. He joined the School of Electrical and Computer Engineering at the Georgia Institute of Technology as an assistant professor in August 2000. His research interests are in wireless network protocols, mobile computing, and network quality of service. He is a member of the IEEE.



**Mary Ann Ingram** received the BEE and PhD degrees from the Georgia Institute of Technology (Georgia Tech) in 1983 and 1989, respectively. From 1983 to 1986, she was a research engineer with the Georgia Tech Research Institute in Atlanta, performing studies on radar electronic countermeasure (ECM) systems. In 1986, she became a graduate research assistant with the School of Electrical and Computer Engineering at Georgia Tech, where, in 1989,

she became a faculty member and is currently an associate professor. Her early research areas were optical communications and radar systems. Since 1997, her research interest has been the application of multiple antenna systems to wireless communications. In particular, she and her students have investigated the use of RF beamformers and RF switches in MIMO and adaptive array architectures, wideband MIMO channel measurement and stochastic modeling, multiantenna architectures for semipassive RF tags and their interrogators, and cross-layer algorithm development for networks with interfering MIMO links. Many of these projects involve the design and construction of hardware prototypes. She is a senior member of the IEEE.



**Tae-Young Chang** received the BS degree in electronic engineering from Korea University in 1999 and the MS degree in telecommunication system technology from the same university in 2001. He is at present a PhD degree student in the School of Electric and Computer Engineering at the Georgia Institute of Technology. He works at the Georgia Tech Networking and Mobile Computing (GNAN) Research Group. His research interests are in wireless networks and mobile computing. He is a student member of the IEEE.

► For more information on this or any other computing topic, please visit our Digital Library at [www.computer.org/publications/dlib](http://www.computer.org/publications/dlib).